Supporting Information

Neuron-Inspired Interpenetrative Network Composed of Cobalt-Phosphorus-Derived Nanoparticles Embedded within Porous Carbon Nanotubes for Efficient Hydrogen Production

*Juanxia Shen, Zhi Yang *, Mengzhan Ge, Ping Li, Huagui Nie, Qiran Cai, Cancan Gu, Keqin Yang, Shaoming Huang **

[*] Dr. Z. Yang, J. Shen, M, Ge, P. Li, H. Nie, C. Gu, K. Yang, Prof. S. Huang
Nanomaterials & Chemistry Key Laboratory, Wenzhou University, Wenzhou, 325027, China
E-mail: yang201079@126.com, smhuang@wzu.edu.cn
Dr. Q. Cai
Institute for Frontier Materials, Deakin University, Waurn Ponds, Victoria, Australia

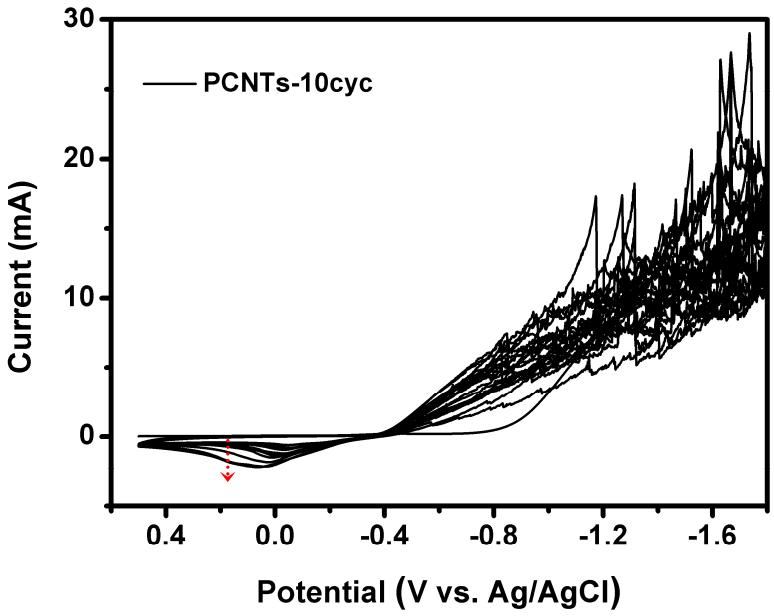

Figure S1. The entire CV curves during the formation of the PCNT-10cyc sample

S2 Ohmic drop correction

The ohmic drop correction was performed with a series resistance (*R*s) determined by electrochemical impedance measurement. The electrochemical impedance spectroscopy was performed from 100 kHz to 10 mHz at an open circuit voltage of 30 mV. In a type example, the resistance of the PCNTs-10cyc sample was determined to be ~9.9 Ω, as shown in the Nyquist plot of Fig. S2. The *iR* correction to data with the series resistance is done by the equation of $\eta_{corr}=\eta_{exp}- iR$.

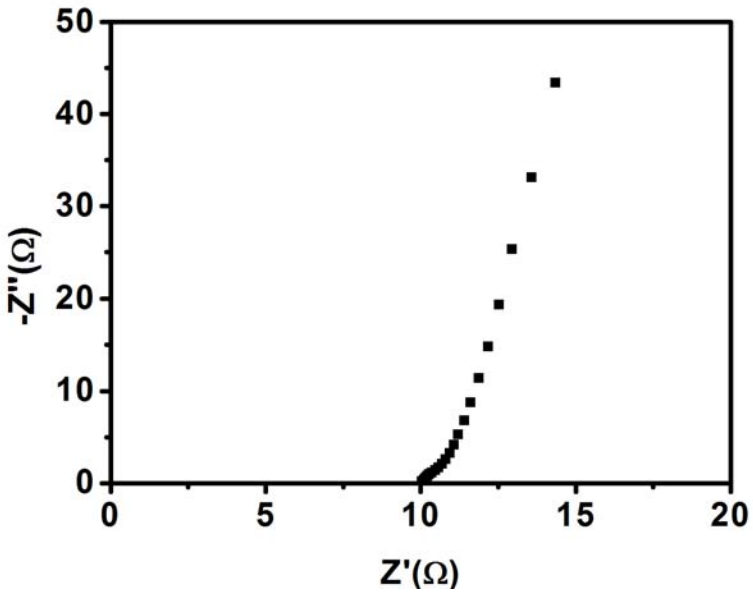

Figure S2. Nyquist plot of the PCNTs-10cyc sample.

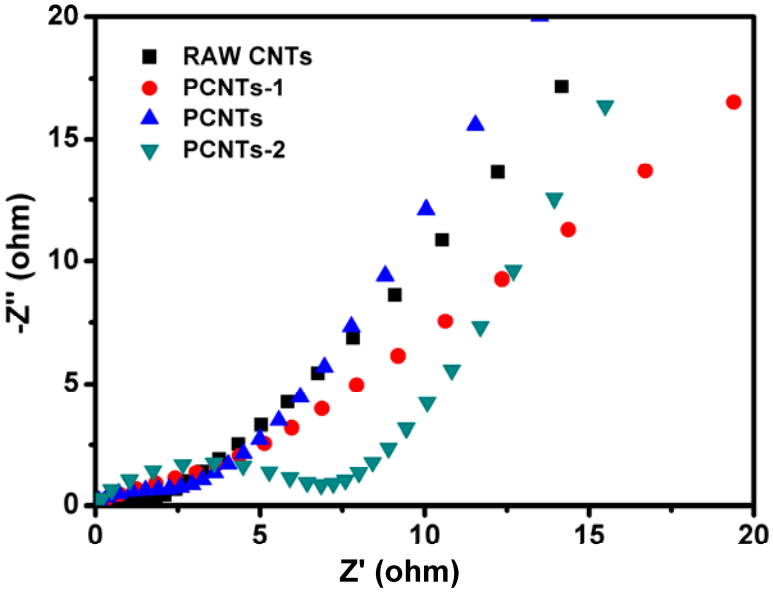

Figure S3. Electrochemical impedance spectra of raw CNTs and PCNTs.

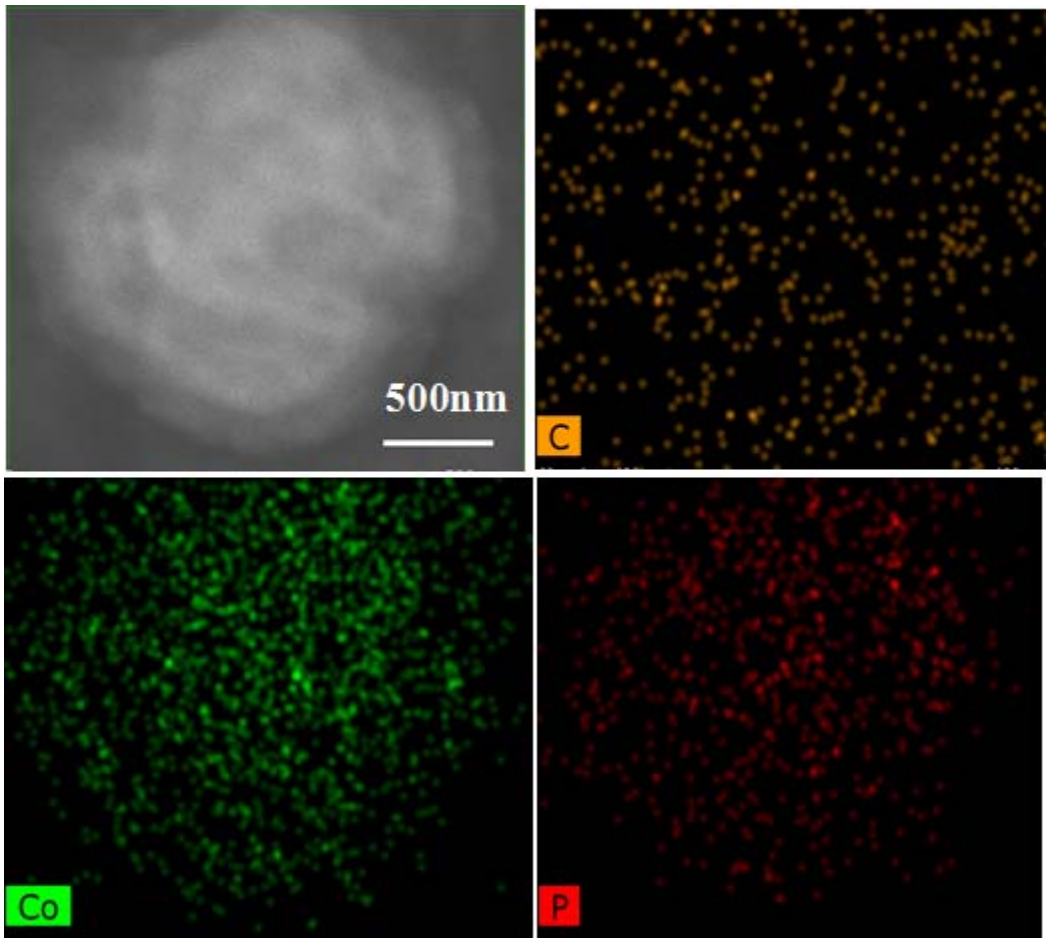

Figure S4. STEM and corresponding element mapping of PCNTs-50cyc.

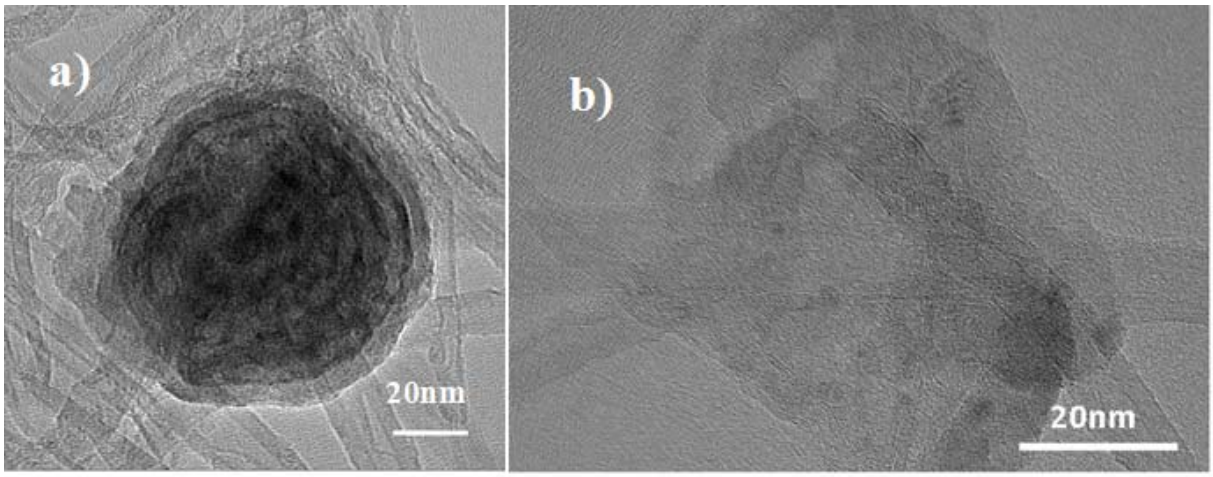

Figure S5. Enlarged TEM image of PCNTs-10cyc.

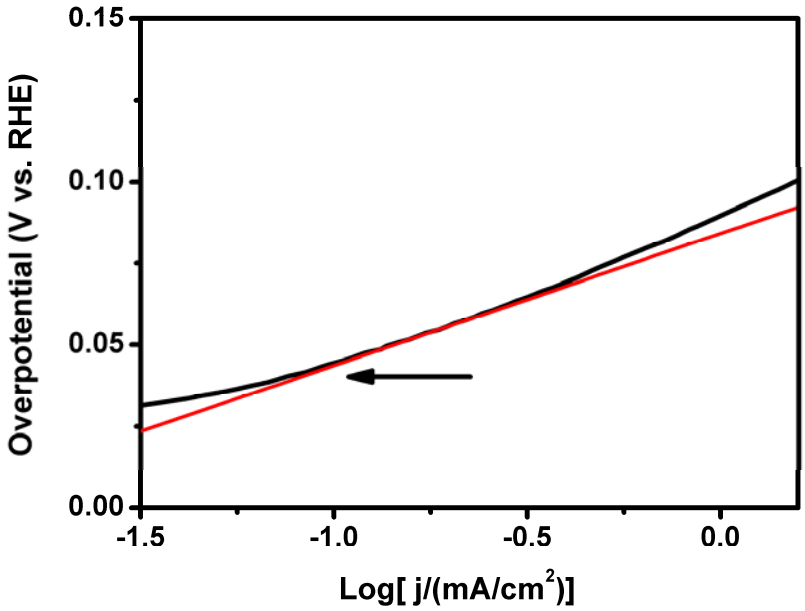

Figure S6. Tafel plot in the region of low current densities of PCNTs-10cyc in 0.5 M H_2SO_4. The onset overpotential is determined by the potential when the plot starts to deviate from the linear region as indicated by the arrow.

Table S1. Comparison of HER performance in acid media for NIN-Co-P/PCNTs nanocomposites with other HER electrocatalysts. ([a] catalysts directly grown on current collectors)

Catalyst	Onset potential (mV)	Tafel slope (mV/dec)	Current density (j, mA/cm^2)	η at the corresponding j (mV)	Exchange current density (mA/cm^2)	TOF(s^{-1})	Ref.
NIN-Co-P/PCNTs	43	40	2 10 20 60	99.5 150.6 177.6 255	1.0×10^{-2}	3.2 η=0.2V	This work
CoP-n^+Si		61	10	202	6.60×10^{-3}	0.48 η=0.1V 1.0 η=0.12V	[1]
CoP	100	76	10 20	226 275	1.9×10^{-2}		[2]
Branched CoP nanostructures		48	20 60	117 145		0.019 η=0.1V	[3]
CoP NPs		87	10	221	5.4×10^{-2}		[4]
Co_2P nanorods	70	71	10 20	134 167		0.725 η=0.143V	[5]
CoP NTs		60	2 10	72 129		1.0 η=0.106V	[6]
CoP/CC	38	51	10 20 60	67 100 165	0.288	0.725 η=0.075V	[7]
CoP/Ti		50	20	95			[8]
Ni_2P NPs		46	20 100	130 180	3.3×10^{-2}	0.50 η=0.2V	[9]
Ni_5P_4		40	10	140			[10]
Ni_2P	170	70	10	346	3.84×10^{-6}	0.025 η=0.1V	[11]
MoP	50	54	30	180	0.034		[12]
Co@NC/NG	49	79.3	13.6	200			[13]
CoS_x		93	2	83			[14]
$[Mo_3S_{13}]^{2-}$ cluster	100-200	40	10	180		3.0 η=0.2V	[15]
MoS_3/FTO[a]	120	40	2 16	170 300	1.3×10^{-4}	0.8 η=0.22V	[16]
Double-gyroid MoS_2/FTO[a]	150-200	50	2	190	6.9×10^{-4}		[17]
Defect-rich MoS_2	120	50	13	200	8.91×10^{-3}	0.7 η=0.3V	[18]
PI/CNT-RGO-MoS_2	90	61	3 13	100 200	1.1×10^{-2}		[19]
Nanostructured MoS_2/CC	100	50	86	250	9.2×10^{-3}		[20]

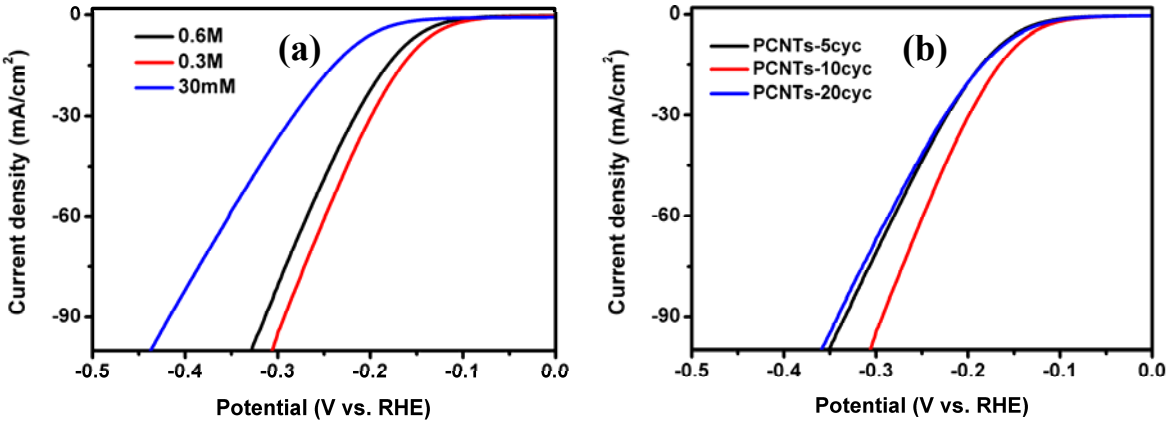

Figure S7. (a) polarization curves for the PCNT-10cyc samples under various precursor concentrations; (b) polarization curves for PCNTs-5cy, PCNTs-10cyc, PCNTs-20cyc samples obtained in 0.3 M $CoSO_4 \cdot 7H_2O$, 0.3M $NaH_2PO_2 \cdot H_2O$ solution containing 0.4 M H_3BO_3.

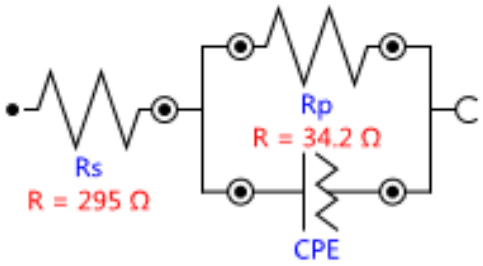

Figure S8. Their electrical equivalent circuit diagram for fitting the solid-liquid interface .

Table S2. The impedance parameters derived by fitting the EIS responses on the NIN-Co-P/PCNTs nanocomposites with various deposition cycles in 5 mM H_2SO_4.

Samples	R_S (Ω)	R_P (Ω)	CPE (μMho)
PCNTs-5cyc	338	39.8	4.66
PCNTs-10cyc	295	34.2	67
PCNTs-20cyc	319	62	9.9

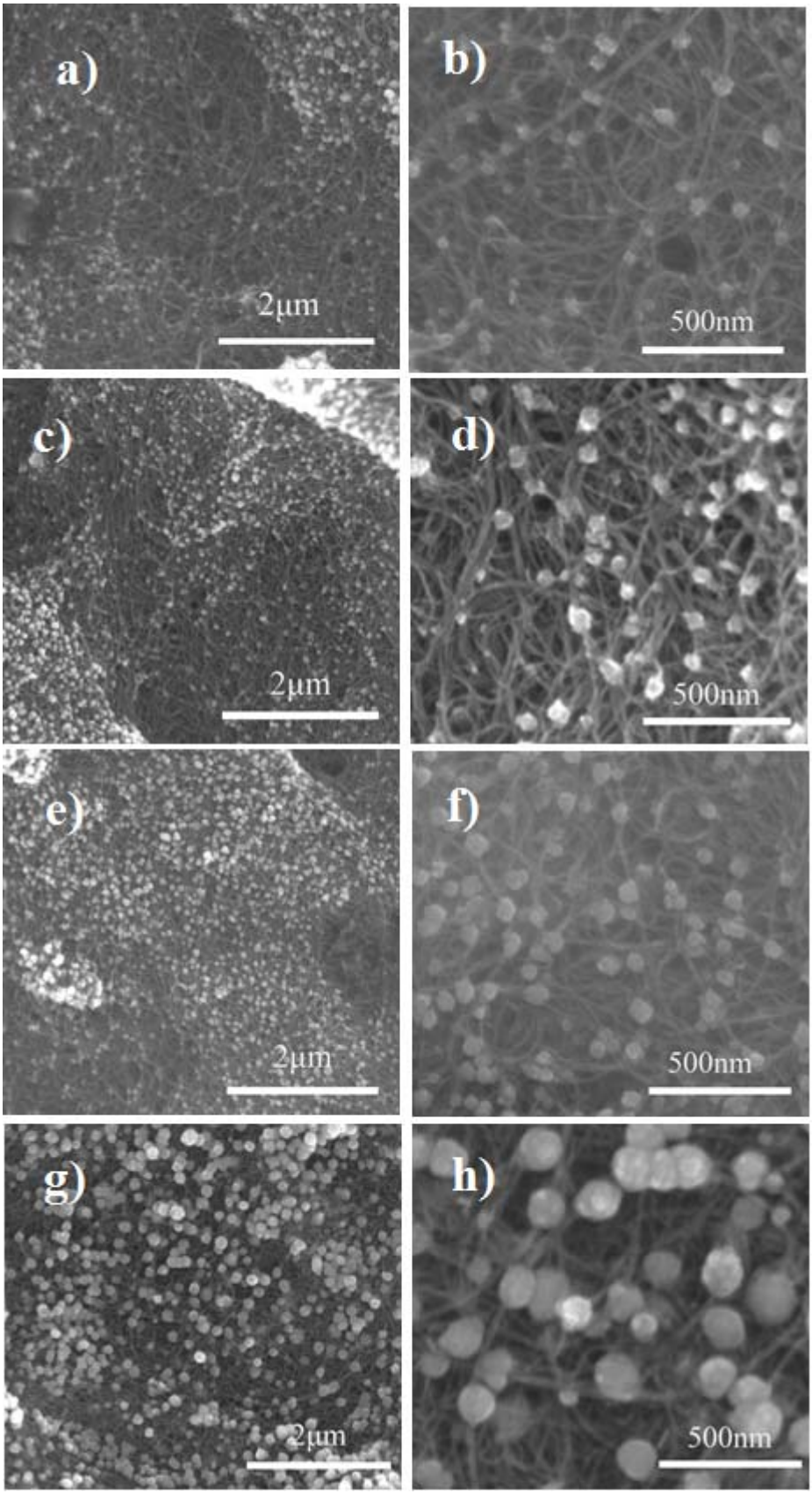

Figure S9. SEM images of (a,b) PCNTs-5cyc, (c,d) PCNTs-10cyc, (e,f) PCNTs-20cyc, (g,h) PCNTs-50cyc.

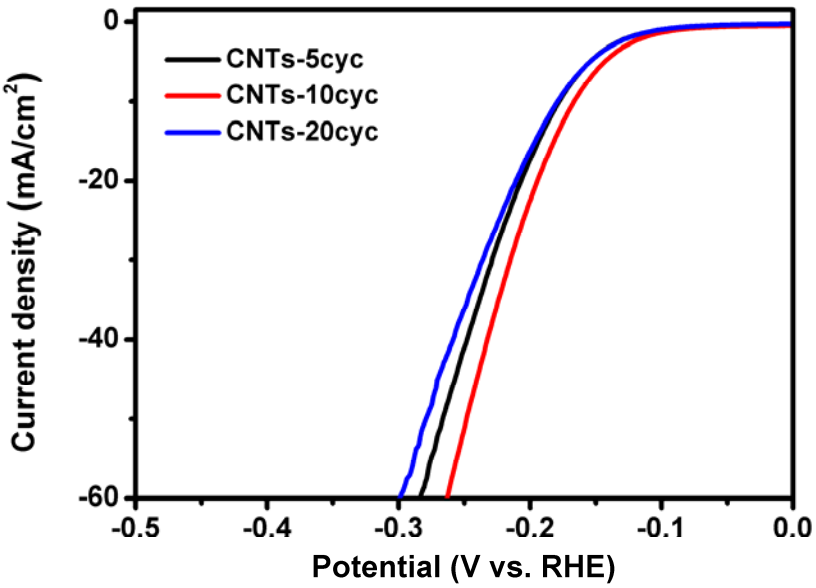

Figure S10. Polarization curves for CNTs-5cyc, CNTs-10cyc, CNTs-20cyc in H_2SO_4 solution (0.5M).

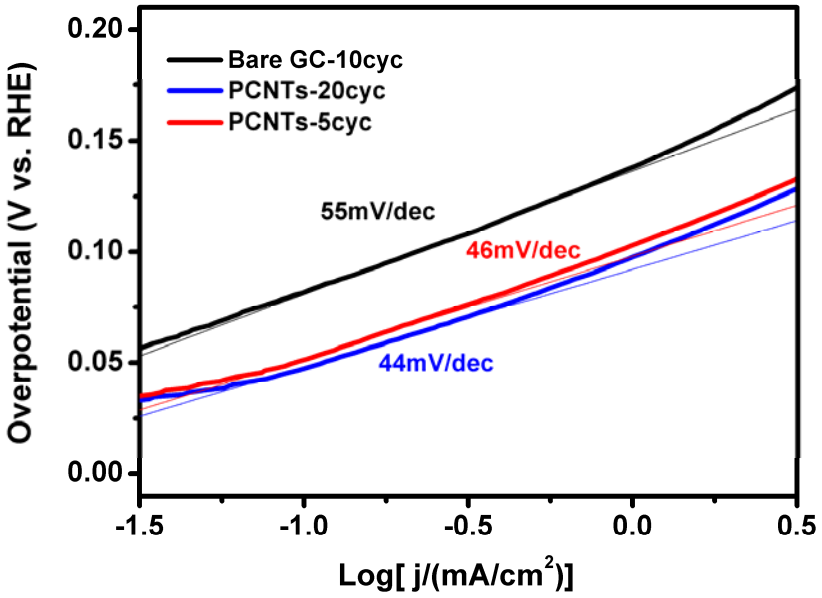

Figure S11. Tafel plots of PCNTs-5cyc, PCNTs-20cyc and Bare GC-10cyc.

S12 Estimation of Turn Over Frequency (TOF)

To estimate the turn over frequency (TOF) for the NIN-Co-P/PCNTs composites catalyst, we adopt the approach that used in Jaramillo et al[21, 22]. First, the potential was swept between 0.10 to 0.30 V vs RHE at each of five different scan rates (20, 40, 80, 160, 200 mV/s) to measure electrochemical capacitance. The cyclic voltammograms can be seen in Figures S11a. We measured the capacitive currents in a potential range where no faradic processes are observed, i.e. at 0.20 V vs RHE. The measured capacitive currents are plotted as a function of scan rate in Figure S11b and a linear fit determined the specific capacitance to be 8.22 mF/cm^2 for PCNTs-10cyc, and 7.61 mF/cm^2 for PCNTs. The specific capacitance can be converted into an electrochemical active surface area (ECSA) using the specific capacitance value for a flat standard with 1 cm^2 of real surface area. The specific capacitance for a flat surface is generally found to be in the range of 20-60 μF cm^{-2}.[22-26] In the following calculations of TOF we assume 40 μF cm^{-2}.

Calculated electrochemical active surface area.

$$A_{ECSA}^{CoP} = \frac{Capaci\tan ce((PCNTs-10cyc)-PCNTs)}{40\mu Fcm^{-2}\,percm_{ECSA}^{-2}}$$

To further access the per-site TOF, we used following formula:

$$TOF\ \ per\ site = \frac{\#Total\ \ Hydrogen\,Turn\ Over/cm^2\ \ geometric\ area}{\#Surface\ Sites(Catalyst)/cm^2\ \ geometric\ area}$$

Surface sites per real surface area

Surface sites =1.948*10^{15}atoms cm$^{-2}_{real}$ [26]

Total number of hydrogen turn over events per geometric area happened at 1mA/cm^2 close to $3.12\times10^{15}\,\frac{H_2/s}{cm^2}$. [26]

So the TOF per site at η = 0.2V (current density of 30.28 mA/cm^2) and pH = 0 is determined as follows.

$$\frac{\left(3.12\times10^{15}\,\frac{H_2/s}{cm^2}\,per\,\frac{mA}{cm^2}\right)\times\left(30.28\,\frac{mA}{cm^2}\right)}{surface\ sites\times A_{ECSA}} = 3.2\,\frac{H_2/s}{surface\ sites}$$

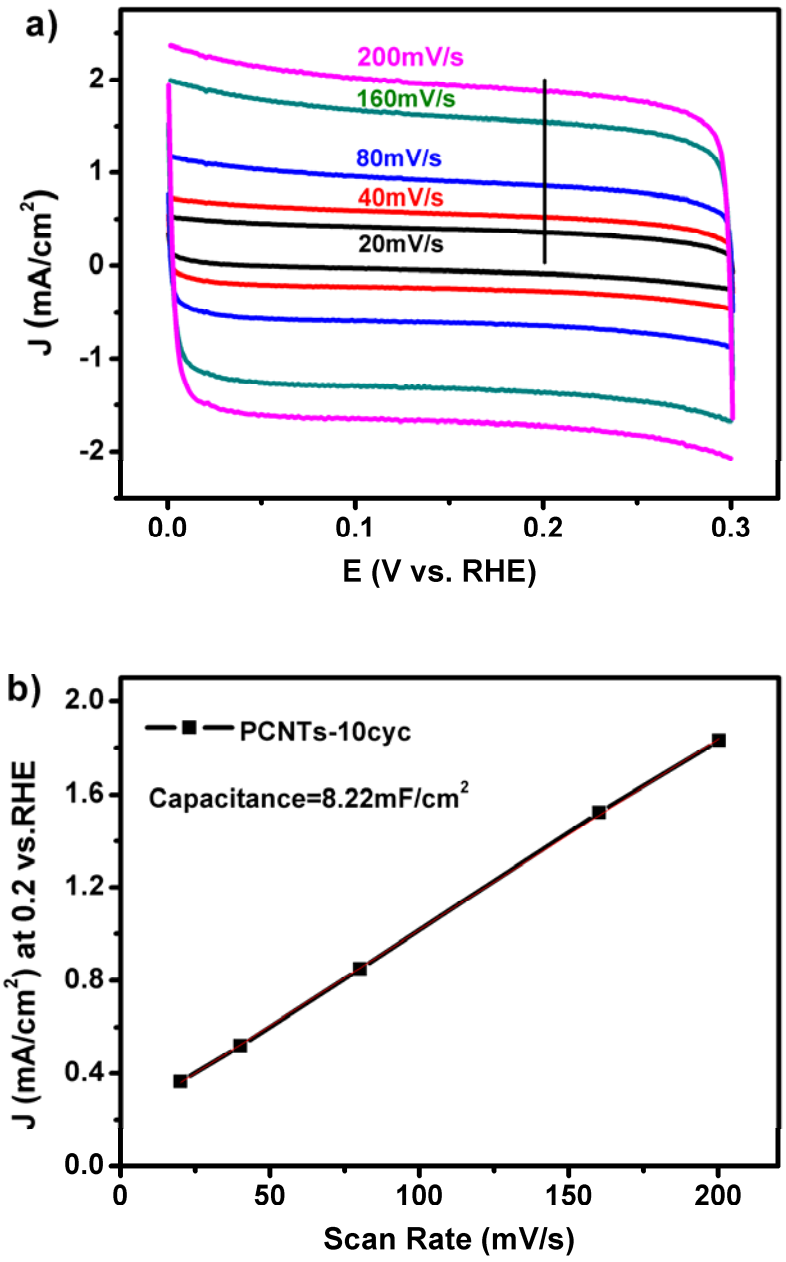

Figure S12. (a) Cyclic voltammetry curves of PCNTs-10cyc in the region of 0-0.3V vs RHE. (b) The differences in current density variation at an overpotential of 0.2V plotted against scan rate fitted to a linear regression enables the estimation of double-layer capacitance.

References

[1] T. R. Hellstern, J. D. Benck, J. Kibsgaard, C. Hahn, T. F. Jaramillo**,** *Adv. Energy Mater.* **2016,** 6, 1501758

[3]**'** J. Kibsgaard, C. Tsai, K. Chan, J. D. Benck, J. K. Nørskov, F. Abild-Pedersen, T. F. Jaramillo *Energy Environ. Sci.***, 2015,** 8, 3022

[2] Q. Liu, J. Tian, W. Cui, P. Jiang, N. Cheng, A. M. Asiri, X. Sun, *Angew. Chem. Int. Ed.* **2014**, *53*, 6710.

[3] E. J. Popczun, C. W. Roske, C. G. Read, J. C. Crompton, J. M. McEnaney, J. F. Callejas, N. S. Lewis, R. E. Schaak, *J. Mater. Chem. A* **2015**, *3*, 5420.

[4] P. Jiang, Q. Liu, C. Ge, W. Cui, Z. Pu, A. M. Asiribc, X. Sun, *J. Mater. Chem. A* **2014**, *2*, 14634.

[5] Z. Huang, Z. Chen, Z. Chen, C. Lv, M. G.Humphrey, C. Zhang, *Nano Energy* **2014**, *9*, 373.

[6] H. Du, Q. Liu, N. Cheng, A. M. Asiri, X. Sun, C. Li, *J. Mater. Chem. A* **2014**, *2*, 14812.

[7] J. Tian, Q. Liu, A. M. Asiri, X. Sun, *J. Am. Chem. Soc.* **2014**, *136* 7587.

[8] E. J. Popczun, C. G. Read, C. W. Roske, N. S. Lewis, R. E. Schaak, *Angew. Chem. Int. Ed.* **2014**, *53*, 5427.

[9] E. J. Popczun, J. R. McKone, C. G. Read, A. J. Biacchi, A. M. Wiltrout, N. S. Lewis, R. E. Schaak, *J. Am. Chem. Soc.* **2013**, *135*, 9267.

[10] M. Ledendecker, S. K. Calderón, C. Papp, H. P. Steinrück, M. Antonietti, M. Shalom, *Angew. Chem. Int. Ed.* **2015**, *54*, 12361.

[11] X. Chen, D. Wang, Z. Wang, P. Zhou, Z. Wu, F. Jiang, *Chem. Commun.* **2014**, *50*, 11683.

[12] P. Xiao, M. A. Sk, L. Thia, X. Ge, R. J. Lim, J. Y. Wang, K. H. Lima, X. Wang, *Energy Environ. Sci.* **2014**, *7*, 2624.

[13] W. Zhou, J. Zhou, Y. Zhou, J. Lu, K. Zhou, L. Yang, Z. Tang, L. Li, S. Chen, *Chem. Mater.* **2015**, *27*, 2026.

[14] N. Kornienko, J. Resasco, N. Becknell, C. M. Jiang, Y. S. Liu, K. Nie, X. Sun, J. Guo, S. R. Leone, P. Yang, *J. Am. Chem. Soc.* **2015**, *137*, 7448.

[15] J. Kibsgaard, T. F. Jaramillo, F. Besenbacher, *Nat. Chem.* **2014**, *6*, 248.

[16] D. Merki, S. Fierro, H. Vrubel, X. Hu, *Chem. Sci.* **2011**, *2*, 1262.

[17] J. Kibsgaard, Z. Chen, B. N. Reinecke, T. F. Jaramillo, *Nat. Mater.* **2012**, *11*, 963.

[18] J. Xie, H. Zhang, S. Li, R. Wang, X. Sun, M. Zhou, J. Zhou, X. W. Lou, Y. Xie, *Adv. Mater.* **2013**, *25*, 5807.

[19] Y. Jiang, X. Li, S. Yu, L. Jia, X. Zhao, C. Wang, *Adv. Funct. Mater.* **2015**, *25*, 2693.

[20] Y. Yan, B.Y. Xia, N. Li, Z. Xu, A. Fisherc, X. Wang, *J. Mater. Chem. A* **2015**, *3*, 131.

[21] J. Kibsgaard,T. F. Jaramillo, *Angew. Chem. Int. Ed.* **2014**, *53*, 14433.

[22] J. Kibsgaard, C. Tsai, K. Chan, J. D. Benck, J. K. Nørskov, F. Abild-Pedersen, T. F. Jaramillo, *Energy Environ. Sci.***, 2015,** 8, 3022

[23] D. C. Grahame, *Chem. Rev*. **1947**, 41, 441.

[24] R. Kötz, M. Carlen, *Electrochim. Acta*, **2000**, 45, 2483.

[25] B. E. Conway, B. V. Tilak, *Electrochim. Acta*, 2002, 47, 3571.

[26] J. D. Benck, Z. B. Chen, L. Y. Kuritzky, A. J. Forman, T. F. Jaramillo, *ACS Catal.*, **2012**, 2, 1916.